20

Differentiation of malignant skin neoplasms using Raman spectroscopy with an excitation wavelength of 532 nm in the High-Wavenumber region

© S.N. Shelygina[1], E.N. Rimskaya[1], A.B. Timurzieva[1,2], I.N. Saraeva[1], K.G. Kudrin[1,3], A.E. Rupasov[1], A.A. Nastulyavichus[1]

[1] Lebedev Physical Institute, Russian Academy of Sciences, 119991 Moscow, Russia
[2] FSSBI „Semashko National Research Institute of Public Health", 105064 Moscow, Russia
[3] Department of Oncology, Radiation Therapy and Reconstructive Surgery, Sechenov University, 119991 Moscow, Russia

e-mail: shelyginasn@lebedev.ru

Received December 11, 2023
Revised January 09, 2024
Accepted January 16, 2024

Confocal scanning Raman and fluorescence microspectroscopy are structure-sensitive optical techniques that allow for the non-invasive analysis of biomarkers in skin tissue. Distinct spectral differences were observed in the Raman spectra of basal cell carcinoma and squamous cell carcinoma compared to healthy skin and papilloma. Our analysis of Raman and fluorescence spectra at an excitation wavelength of 532 nm enabled us to propose two spectral criteria: intensity ratios for the bands at 2880 and 1445 cm^{-1}, and for the bands at 2930 and 1445 cm^{-1}. These criteria are based on differences in cell membrane lipid fluctuations, which serve as biomarkers. They allowed for the differentiation of healthy skin from basal cell carcinoma, squamous cell carcinoma, and papilloma with a sensitivity and specificity of more than 90%, demonstrating high clinical significance in the differential diagnosis of skin neoplasms.

Keywords: Raman and photoluminescence microspectroscopy, skin cancer, non-invasive diagnostic, spectral analysis.

DOI: 10.61011/0000000000

Introduction

Skin cancer morbidity is growing every year. Morbidity growth is probably connected with ultraviolet exposure, increased outdoor activities, changing style of dress, increase in life expectancy, depletion of ozone layer, genetics, etc.

Basal cell skin carcinoma (BCC) and squamous cell skin carcinoma (SCC) are the most widespread types of nonmelanoma malignant neoplasms in the world, therefore their early non-invasive diagnostics is a socially important issue. BCC is the most frequent type which usually grows slowly and is locally invasive. SCC is the second most frequent type of nonmelanoma skin cancer that accounts for about 20% to 30% cases [1–3].

Histopathology of the removed material is a traditional „gold standard" of cancer detection. Disadvantages of the method include invasiveness, stringent requirements for medical personnel qualification and time expenditures [4–7]. Non-invasive examination methods, i.e. dermatoscopy, confocal microscopy, multispectral visualization and optical coherent tomography, have certain restrictions [8–10].

Dermatoscopy is a non-invasive visual examination method that is useful to detect skin malignancies at early stages. Sensitivity and specificity of the technique are 93.7% and 87.8%, respectively. Limitation of the technique include a shallow visualization depth (deris level), image resolution and high personnel qualification requirements [11]. Confocal reflection microscopy provides images with high resolution that is close to histologic resolution, but is limited to a depth of 200−300 μm (corresponding to the papillary dermis) [12].

Multispectral visualization uses a portable scanner that makes 10 digital multispectral images in the visible to near IR wavelength range (430−950 nm), the emission penetrates the skin to about 2.5 mm. The technique has high sensitivity — 98.3%, but low specificity — 9.9%, therefore, it is used as pre-biopsy examination [13].

Optical coherent tomography based on low-coherent near-IR wavelength interferometry (700−1300 nm), ensures skin visualization with high (close to histologic) spatial resolution equal to several micrometers and a penetration depth of 1−3 mm. The technique provides structural visualization of bio-tissues, blood microcirculation visualization without using contrast agents, therefore it is of high demand in a number of medical applications [14]. However, the technique does not distinguish individual cells [15–17].

Multimodal methods demonstrate high sensitivity and specificity performance. For example, [18] offers a machine learning algorithm based on the classification data on various types of BCC and benign neoplasms *in vivo* (obtained using a multimodal screening method that combines diffuse reflectance spectroscopy, optical coherent tomography

and high-frequency ultrasound). The algorithm ensures a sensitivity of $70.6 \pm 17.3\%$, specificity of $95.9 \pm 2.5\%$, accuracy of $72.6 \pm 14.2\%$. For differentiation of basalioma and benign neoplasms without considering the clinical form, the technique achieves a sensitivity of $89.1 \pm 8.0\%$ and specificity of $95.1 \pm 0.7\%$.

The Raman scattering spectroscopy (RS) has the potential to detect and study the evolution of human malignancies both *in vitro* and *in vivo* in esophagus, stomach, lungs, prostate, arteries and on skin [19–22]. The method has high sensitivity and specificity (95%) for skin neoplasm detection [23]. The RS confocal spectroscopy analyses the material at various depths. Thus, [24] investigates melanin distribution in skin by the RS microspectroscopy at excitation wavelengths of 785 and 671 nm and a depth up to $60\,\mu$m. In [25], water content in pig skin at a depth up to $200\,\mu$m is investigated *ex vivo* by the confocal RS microspectroscopy at an excitation wavelength of 671 nm.

Laser emission at various wavelengths has various skin penetration depths, that is also useful for the analysis of tissue composition at various depths [26]. In [27], *in vivo* examination of skin neoplasms was carried out using a 785 nm portable RS spectrometer by means of analysis of RS spectra combination and near-IR autofluorescence (AF) ($300-1800\,\mathrm{cm}^{-1}$). Spectroscopy data analysis was conducted using PLS-DA. The use of RS signal together with AF demonstrate the best results in melanoma and pigmented neoplasm differentiation (seborrheic keratosis and nevuses: sensitivity and specificity are 90% and 26%, melanoma and seborrheic keratosis: sensitivity and specificity are 90% and $> 40\%$, as well as malignant and benign neoplasms: sensitivity and specificity are 90 and 32). Accuracy of this approach is lower than for deep-freeze instruments and or experience dermatologists, but increases accuracy for general practitioners and resident physicians.

Surface-enhanced RS spectroscopy is being widely developed for biomedicine applications. For example, [28] describes a ratiometric surface-enhanced RS spectroscopy (SETRS) method for *in vivo* non-invasive localization and perioperative navigation of deep sentinel lymph node in living rats. Ultra-bright SERS-active nanoparticles are used for RS signal enhancement. The method provides accurate measurement of phantom damage in rat tissues *ex vivo* with mean absolute error 11.8% and achieves accurate localization of a popliteal lymph node of a rat at a depth of 6 mm.

In our previous study [29], we have investigated the RS and fluorescent (FL) microspectroscopy method at excitation wavelengths 532, 785 and 1064 nm for *in vitro* detection of various skin malignancies. Clear differences in RS spectra were detected in the range from 900 to $1800\,\mathrm{cm}^{-1}$ BCC and SCC compared with normal skin. We had offered two new spectral criteria that do not depend on the wavelength (intensity ratios for 1302 and $1445\,\mathrm{cm}^{-1}$, 1745 and $1445\,\mathrm{cm}^{-1}$ bands) and are associated with characteristic stretching of membrane lipids that was confirmed by the multivariate curve resolution (MCR) method. The criteria were used to differentiate normal skin, BCC and SCC with sensitivity and specificity more than 95%.

RS band explanation within $2850-3061\,\mathrm{cm}^{-1}$

Wave number, cm^{-1}	Assignment	Reference No.
2850	Symmetric CH_2-stretching of lipids and fatty acids	[30]
2876–2919	Asymmetric CH_2-stretching of lipids and proteins	[30]
2929–2940	Symmetric CH_2-stretching primarily of proteins and lipids	[33]
3005	Stretching of water molecules, closely connected with hydrogen (DAA–OH, single donor, double acceptor)	[25,31]
3059–3061	CH stretching of aliphatic and olefinic groups of lipids	[34]

In the above mentioned study, analysis was carried out in the spectral range of $900-1800\,\mathrm{cm}^{-1}$ — a so-called „fingerprint“ region. A spectral range of higher wavelengths $2800-3100\,\mathrm{cm}^{-1}$ provides additional information and also may be of practical interest for tissue examination and biomarker search. Herein, we used the RS/FL microspectroscopy method to test the spectral range of $2800-3100\,\mathrm{cm}^{-1}$ for characteristic biomarkers for *in vitro* examination of malignant and benign neoplasms.

Experimental

Fresh tissue samples were taken from patients during surgical operations. Immediately after tumor tissue removal, small tissue fragments up to 3×3 mm in size, that included a tumor area within the surrounding non-damaged tissue, were taken from the samples. The samples were placed in tightly sealed tubes with saline and unique number. The test material was taken in such a way as to avoid distortion of their further histologic examination. The period from the time of sampling to the start of spectra recording was maximum 1.5 h.

The study analyzed RS/FL spectra gathered by scanning 7 BCC samples, 5 SCC samples (for each tumor sample, a signal from the surrounding normal tissue was also recorded), 3 papilloma samples (benign neoplasm) and 15 normal skin samples from different patients (approximately equal to the number of men and women aged 30–60). According to the microscopic biopsy data, all BCC and SCC cases were

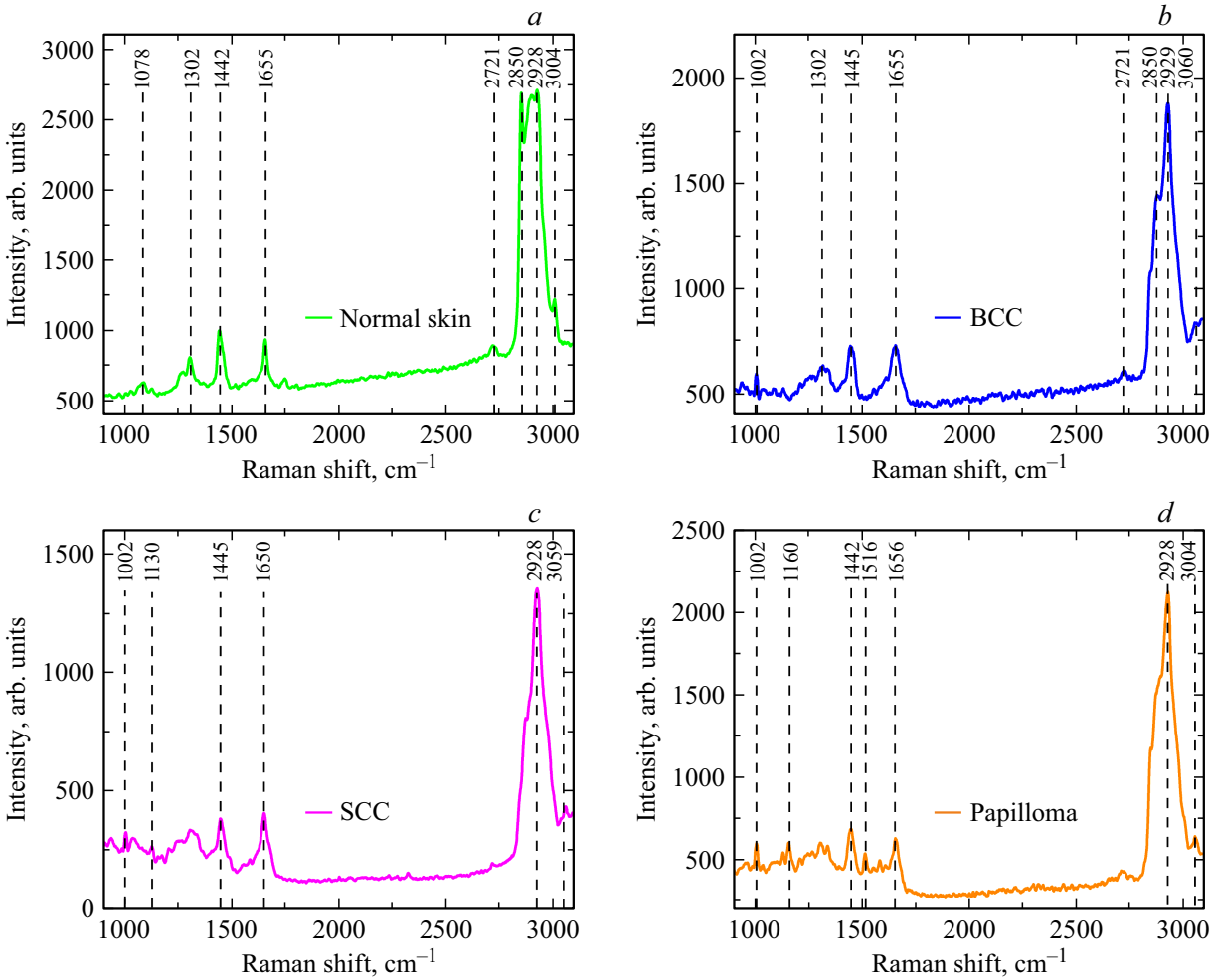

Figure 1. Initial RS/FL spectra at an excitation wavelength of 532 nm for normal skin (*a*), BCC (*b*), SCC (*c*) and papilloma (*d*).

classified as early-stage tumors (cancer stage: G1 (well differentiated) and G2 (moderatelly differentiated)).

The RS/FL sample spectra were recorded by 2D RS/FL scanning confocal microspectroscopy using Confotec MR520 spectromicroscope (SOL instruments, Minsk, Belarus) with a excitation wavelength of 532 nm at room temperature (25°C). Laser emission was focused on the sample surface by N Plan 50/0.50 lens (Leica, Germany), backscatter was collected by the same lens. The spectra were recorded at exposure time 2 s, laser emission power in the sample plane was lower than 20 mW, beam diameter was $\sim 1\,\mu$m. In order to cover the maximum sample area, RS/FL spectra with 10–20 independent areas of each sample were taken.

FL contribution in the range of 900–3100 cm^{-1} was subtracted from the initial spectra based on the Vancouver algorithm that is the best one for biomedical samples. Each spectrum was smoothed by the Savitzky-Golay method. Then all RS spectra with removed FL in the range from 900 to 3100 cm^{-1} were normalized to the 1442 cm^{-1} band intensity that corresponds to CH_2 stretching of proteins and lipids and is more stable, because different groups of patients have different substance concentration in tissues.

Results and discussion

Spectral range of large wave numbers 2800–3550 cm^{-1} contains CH stretch of proteins and lipids in the range of 2700–3100 cm^{-1}, symmetric NH stretch of proteins is at 3329 cm^{-1}, OH stretch of water is at 3350–3550 cm^{-1} [30]. Detail ed explanation is given in the table. This range relies less on the FL contribution than the „fingerprint“ range.

RS/FL spectrum provides information about morphological structure of tissue. Figure 1 shows initial RS/FL spectra within 900–3100 cm^{-1} for normal skin, BCC, SCC and papilloma samples at an excitation wavelength of 532 nm. RS spectral bands correspond to various molecular components of skin. Wave numbers of RS base bands in a high wave number range from 2500 to 3100 cm^{-1} for normal skin: 2721, 2850, 2881, 2928, 3004, 3062 cm^{-1}, for BCC: 2721, 2850, 2876, 2929, 3063 cm^{-1}, for SCC: 2722,

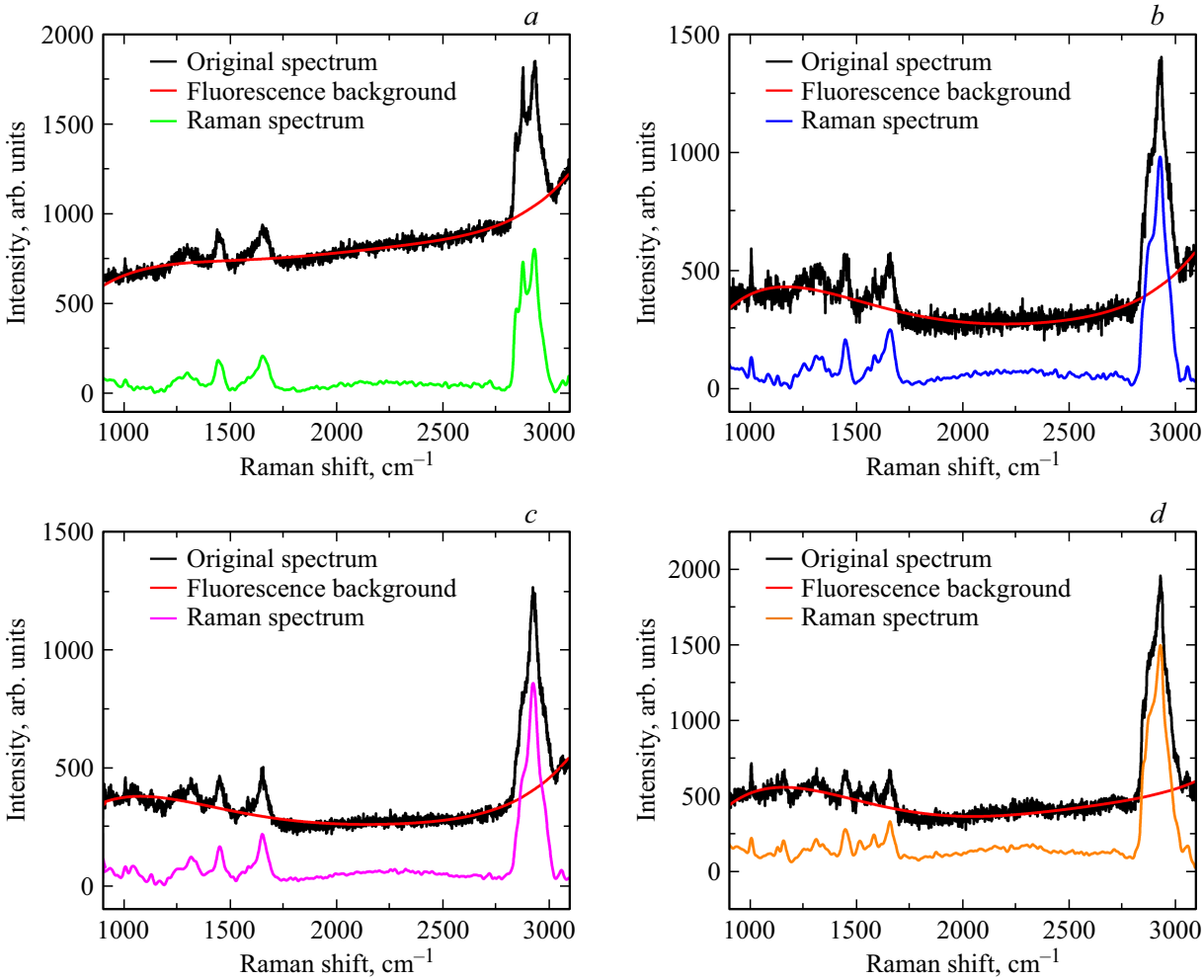

Figure 2. Initial RS/FL spectrum, FL signal spectrum and RS spectrum at an excitation wavelength of 532 nm for normal skin (*a*), BCC (*b*), SCC (*c*) and papilloma (*d*).

2846, 2869, 2928, 3059 cm^{-1} and for papillomas: 2850, 2879, 2931, 3058 cm^{-1}.

The spectra recorded at an excitation wavelength of 532 nm have high FL level that must be subtracted for correct data analysis. The Vancouver algorithm is most widely used for FL signal subtraction in biological tissue measurements [31]. After FL signal subtraction, the spectrum was normalized to the 1445 cm^{-1} RS band intensity. The 1445 cm^{-1} band associated with CH_2 strain of proteins and lipids [30] is relatively nonsensitive to conformation, is typical for RS spectra of both normal skin and neoplasms, therefore it was offered as an intensity standard. An example of FL signal subtraction using the Vancouver algorithm and recorded RS spectra smoothed by the Savitzky–Golay method and normalized to the 1445 cm^{-1} band intensity are shown in Figure 2.

RS spectra within 2700–3100 cm^{-1} after FL signal subtraction, smoothing and division by the 1445 cm^{-1} band intensity are shown in Figure 3. RS spectra represent a set of superimposed stretch bands mainly of CH groups of proteins and lipids.

In contrast to the tumor samples, in the normal skin spectrum, 2850 cm^{-1} stretch corresponding to CH_2 stretch of lipids and fatty acids is resolved [29], as well as 3004 cm^{-1} stretch is present that corresponds to the water molecule stretching closely connected with hydrogen (DAA–OH) [25,31].

In RS spectra of SCC and papillomas, 2928 and 2931 cm^{-1} bands corresponding to CH_2 stretch of proteins and lipids are resolved [32]. In RS spectrum of BCC, 2876 and 2929 cm^{-1} stretch bands corresponding to asymmetric CH_2stretching of lipids and proteins are resolved. The 2850 cm^{-1} band corresponding to fats is weakly resolved. All four samples also have 3059–3061 cm^{-1} bands corresponding to CH stretching of aliphatic and olefinic groups of lipids [34].

Thus, the RS spectra of normal skin and tumors differ in the band intensity ratio corresponding to CH_2 stretching of proteins and lipids and in the presence of water molecule stretch closely connected with hydrogen (DAA–OH) with a wave number of 3004 cm^{-1} in the normal skin spectrum [25,31].

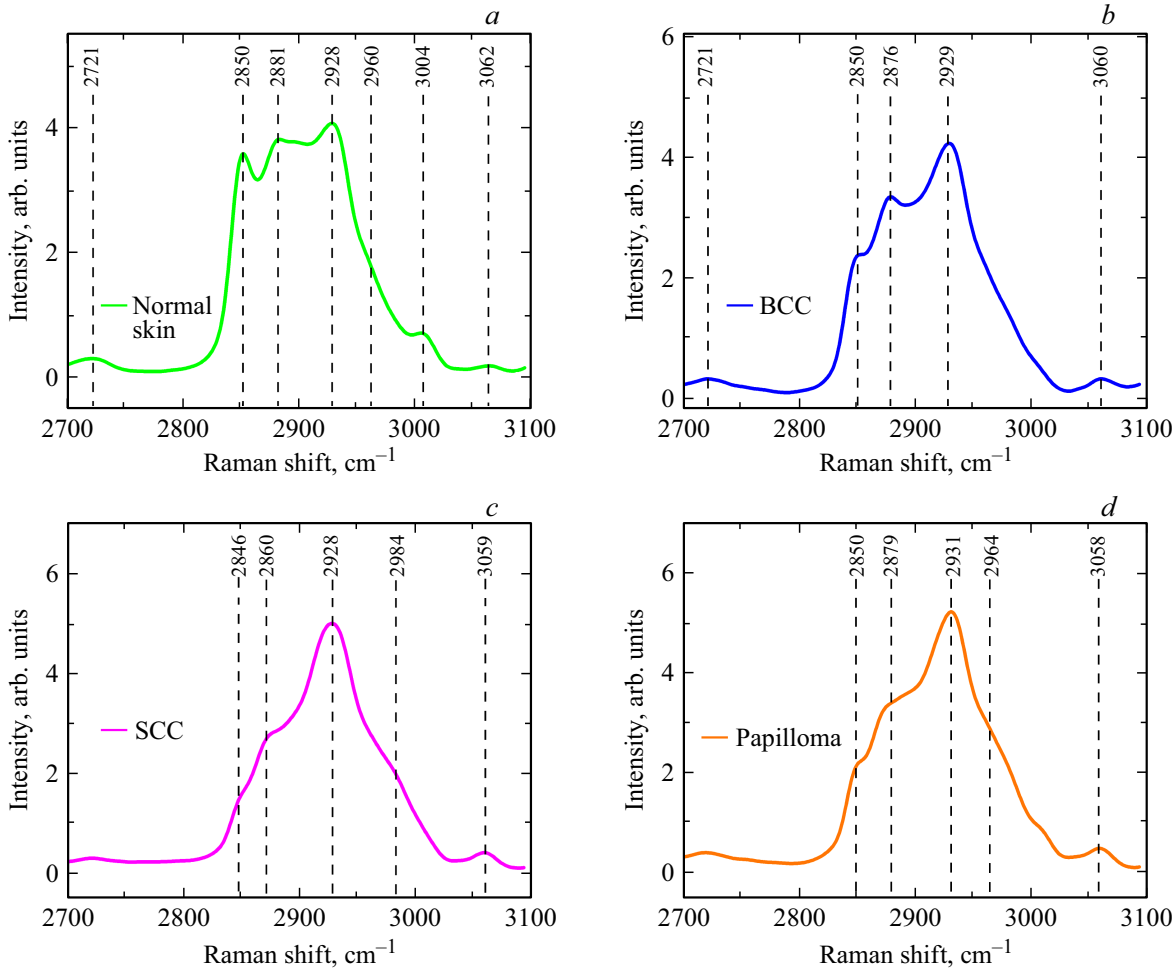

Figure 3. Normalized RS spectra at an excitation wavelength of 532 nm for normal skin (*a*), BCC (*b*), SCC (*c*) and papilloma (*d*) within 2700–3100 cm^{-1}. Values of bands [25,30–34].

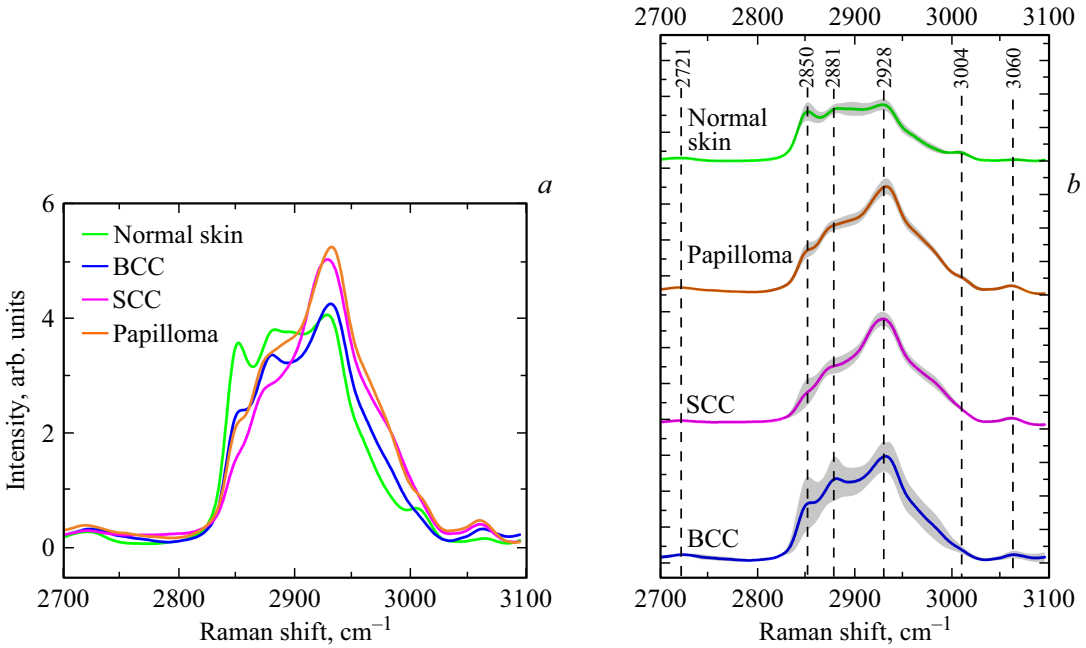

Figure 4. Normalized RS spectra at an excitation wavelength of 532 nm or normal skin, SCC, BCC and papillomas (*a*) with standard deviation intervals (gray regions) (*b*).

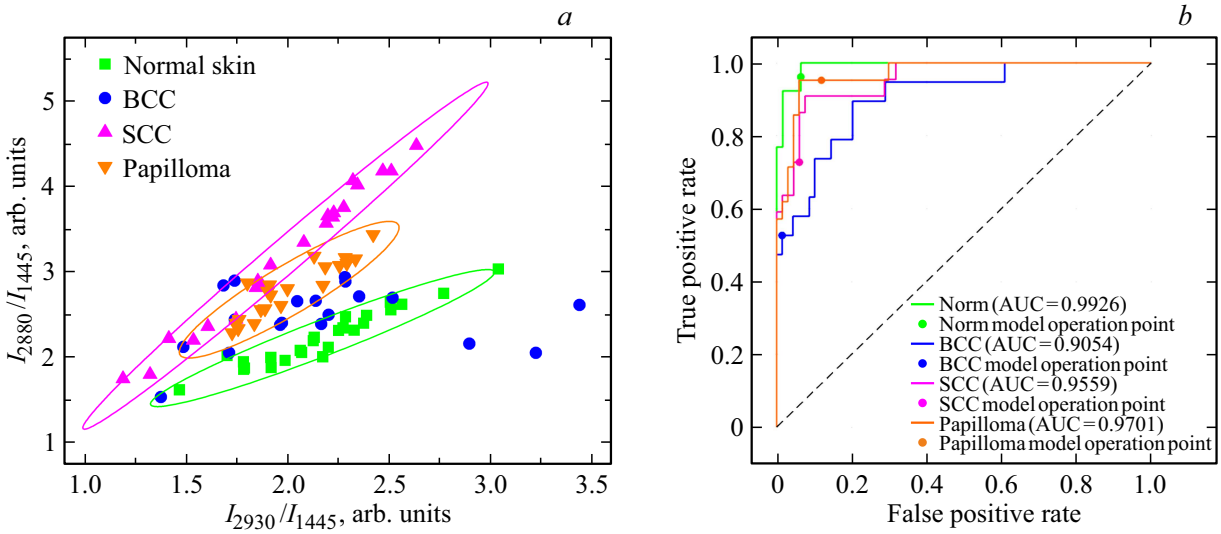

c

	Normal skin	BCC	SCC	Papilloma
Normal skin	96.2	3.8		
BCC	15.8	52.6	15.8	15.8
SCC	4.5		72.7	22.7
Papilloma			4.8	95.2

Figure 5. Classification of normal skin, BCC, SCC and papilloma samples *in vitro* during 532 nm laser excitation using the quadratic discriminant analysis (*a*); ROC curves with AUC values for normal skin, BCC, SCC and papilloma (*b*); confusion matrix in percentage for all data (*c*).

Normalized RS spectra with standard deviation (gray regions) are shown in Figure 4. Wider standard deviation intervals in particular ranges indicate higher variability of individual properties of samples taken from different patients and property distribution across each sample. The widest standard deviation intervals are observed for the RS spectra of normal skin for 2850, 2881 and 2928 cm^{-1} and of BCC for 2850, 2876 and 2929 cm^{-1}. standard deviation for the RS spectrum of BCC is higher than for normal skin. The RS spectra of SCC and papillomas demonstrate smaller standard deviation intervals for 2846, 2869, 2928 and 2850 cm^{-1}, 2879 and 2931 cm^{-1}, respectively.

Spectral criteria for differential diagnostics

Differences in RS spectra of normal skin and tumors allow to differentiate these tissues using the RS/FL microspectroscopy. Herein, we offer a method for differentiation of various skin tumors based on the spectral criterium of RS spectral band intensity ratio of various tissue components. Since the combination of RS and FL signal spectra was reported to increase the sensitivity and specificity of tumor detection, criteria were calculated for the RS spectra with FL signal and spectra without FL signal subtraction and results were compared. In this case, the following spectral criteria were chosen: ratio of $I_{2880/1445}$ and $I_{2930/1445}$ that are defined as RS intensity peak in 2875–2885 cm^{-1} and 2925–2935 cm^{-1} to RS intensity peak in 1440–1450 cm^{-1}:

$$I_{2880/1445} = I_{2880}/I_{1445} \text{ and } I_{2930/1445} = I_{2930}/I_{1445}.$$

The spectral bands were chosen in accordance with the RS spectrum of normal skin. These ratios in coordinates$I_{2880/1445}$ and $I_{2930/1445}$ demonstrate dot clusters for normal skin, BCC, SCC and papilloma. The 1445 cm^{-1} band corresponding to strain CH_2stretch of proteins and

lipids is not sensitive to conformations, is present in all tissue samples and is assumed as intensity standard. The $2880\,cm^{-1}$ band is assigned to symmetric CH_2 stretch of lipids and proteins. The $2930\,cm^{-1}$ band is assigned to CH_2 stretch of lipids and proteins.

Classification performance was assessed using the cross check setup in MATLAB Classification Learner (R2022b, MathWorks, Natick, Massachusetts, USA) and was represented by classification matrices and ROC curves. This allowed the similarity and difference between the tissue samples to be assessed and the sample to be separated using the discriminant analysis.

Figure 5, *a* shows the spectral criteria distribution and calculated boundaries between normal skin, benign (papillomas) and malignant skin neoplasms (BCC and SCC). ROC curves for four classes of tissue samples (Figure 5, *b*) reflect the ratio of true positive results and false positive result for each class. In addition, ROC AUC data (area under curve) were calculated as performance indicator. Thus, ROC AUC values for quadratic discriminant analysis of normal skin, BCC, SCC and papillomas were equal to 0.99, 0.90, 0.95 and 0.97. Classification rates using the quadratic discriminant analysis of normal skin was equal to 96.2%, for SCC — to 72.7% and or papilloma — to 95.2%. For BCC, the indicator was substantially lower and equal to 52.6%, and, therefor, separation of BCC and normal skin tissue is hindered.

From the expert point of view, it is interesting to assess the accuracy of classification of all tumors compared with normal skin. Sensitivity and specificity of the quadratic discriminant analysis were equal to 96% and 90% that is a very good result for differential diagnostics o tumors.

Conclusion

Herein, RS analysis *in vitro* of normal skin, BCC, SCC and papilloma was carried out using the RS and FL scanning at an excitation wavelength of 532 nm within $2800-3100\,cm^{-1}$. After unified procedures for baseline correction and smoothing, the recorded RS spectra looked quite alike, their principal strong bands corresponded to various membrane lipid vibration modes selected as biomarkers. Their intensity ratio demonstrated clear differentiation between normal skin, malignant and benign skin neoplasms.

In particular, using the 532 nm excitation wavelength, we achieved reliable identification of normal skin, BCC, SCC and papillomas for which the classification rates were equal to 96.2, 52.6, 72.7 and 95.2%, respectively. Sensitivity (96%) and specificity (90%) during detection of all tumors (compared with normal skin) were equivalent to the results obtained by expert dermatologists in differentiation of tumors and by other methods (thermometry, ultrasonic skin scanning, cross-polarized optical coherence tomography, terahertz spectroscopy and visualization).

Compliance with ethical standards

The study was carried out in accordance with the Declaration of Helsinki and approved by the Inter-University Ethics Committee of A.I. Yevdokimov Moscow State University of Medicine and Dentistry, Ministry of Health of the Russian Federation (Moscow, Russia, report code 3, 16.03.2023) for human research. Informed consent was received rom all research participants.

Funding

The authors are grateful to the Russian Science Foundation for the financial support of the research within project № 23-25-00249.

Conflict of interest

The authors declare that they have no conflict of interest.

References

[1] T. Diepgen, V. Mahler. Br.J. Dermatol., **146** (61), 1–6 (2002). DOI: 10.1046/j.1365-2133.146.s61.2.x
[2] V. Madan, J.T. Lear, R.M. Szeimies. Lancet, **375** (9715), 673–85 (2010). DOI: 10.1016/S0140-6736(09)61196-X
[3] O. Jones, C. Ranmuthu, P.N. Hall, G. Funston, F.M. Walter. Adv Ther., **37** (1), 603–616 (2020). DOI: 10.1007/s12325-019-01130-1
[4] *Handbook of Optical Biomedical Diagnostics*, ed. by V.V. Tuchin, 2nd ed. (SPIE Press: Bellingham, WA, USA, 2016).
[5] P. Gerami, J.P. Alsobrook, T.J. Palmer, H.S. Robin. J. Am. Acad. Dermatol., **71** (2), 237–44 (2014). DOI: 10.1016/j.jaad.2014.04.042
[6] L.K. Ferris, B. Jansen, J. Ho, K.J. Busam, K. Gross, D.D. Hansen, J.P. Alsobrook 2nd, Z. Yao, G.L. Peck, P. Gerami. JAMA Dermatol., **153** (7), 675–80 (2017). DOI: 10.1001/jamadermatol.2017.0473
[7] C.J. Cockerell, J. Tschen, S.D. Billings, C. Rock, B. Evans, L. Clarke. J. Am. Acad. Dermatol., **72** (5), AB3–AB3 (2015). DOI: 10.1016/j.jaad.2015.02.020
[8] H. Skvara, L. Teban, M. Fiebiger, M. Binder, H. Kittler. Arch. Dermatol., **141** (2), 155–160 (2005).
[9] H.D. Heibel, L. Hooey, C.J. Cockerell. Am. J. Clin. Dermatol., **21** (4), 513–524 (2020). DOI: 10.1007/s40257-020-00517-z
[10] *Handbook of Non-Invasive Methods and the Skin*, 2nd ed., ed. by J. Serup, G.B.E. Jemec, G.L. Grove (CRC Press: Boca Raton, FL, USA, 2006).
[11] N.N. Potekaev, E.K. Shuginina, T.S. Kuzmina, L.S. Arutyunyan. *Dermatoskopiya v klinicheskoy praktike. Rukovodstvo dlya vrachey* (MDV, M.,2011) (in Rissian).
[12] A. Haroon, S. Shaf, B.K. Rao. Dermatol. Clin., **35** (4), 457–64 (2017). DOI: 10.1016/j.det.2017.06.007
[13] G. Monheit, A.B. Cognetta, L. Ferris, H. Rabinovitz, K. Gross, M. Martini, J.M Grichnik, M. Mihm, V.G. Prieto, P. Googe, R. King, A. Toledano, N. Kabelev, M. Wojton, D. Gutkowicz-Krusin. Arch. Dermatol., **147** (2), 188–94 (2011). DOI: 10.1001/archdermatol.2010.302

[14] L. Matveev, V. Zaitsev, G. Gelikonov, A. Matveyev, A. Moiseev, S. Ksenofontov, V. Gelikonov, M. Sirotkina, N. Gladkova, V. Demidov, A. Vitkin. Optics Lett., **40** (7), 1472–1475 (2015). DOI: 10.1364/OL.40.001472
[15] S.A. Alawi, M. Kuck, C. Wahrlich, S. Batz, G. Mckenzie, J.W. Fluhr, J. Lademann, M. Ulrich. Exp. Dermatol., **22** (8), 547–51 (2013). DOI: 10.1111/exd.12196
[16] L. Themstrup, C.A. Banzhaf, M. Mogensen, G.B.E. Jemec. Photodiagn Photodyn Ther., **11** (1), 7–12 (2014). DOI: 10.1016/j.pdpdt.2013.11.003
[17] *Multimodal optical diagnostics of cancer, ed. by V.V. Tuchin, J. Popp, V.P. Zakharov*, (Springer Nature Switzerland AG, Basel, 2020).
[18] Y. Surkov, I. Serebryakova, Y. Kuzinova, O. Konopatskova, D. Safronov, S. Kapralov, E. Genina, V. Tuchin. Diagnostics, **14** (2), 202 (2024). DOI: 10.3390/diagnostics14020202
[19] C. Kendall, J. Hutchings, H. Barr, N. Shepherd, N. Stone. Faraday Discuss, **149** (1), 279–90 (2011). DOI: 10.1039/c005379a
[20] Z. Huang, S.K. Teh, W. Zheng, K. Lin, K. Y. Ho, M. Teh, K.G. Yeoh. Biosens Bioelectron, **26** (2), 383–9 (2010). DOI: 10.1016/j.bios.2010.07.125
[21] N.D. Magee, J.R. Beattie, C. Carland, R. Davis, K. McManus, I. Bradbury, D.A. Fennell, P.W. Hamilton, M. Ennis, J.J. McGarvey, J.S. Elborn. J. Biomed. Opt., **15** (2), 026015 (2010). DOI: 10.1117/1.3323088
[22] J.F. Brennan, T.J. Romer, R.S. Lees, A.M. Tercyak, J.R. Kramer Jr., M.S. Feld. Circulation, **96** (1), 99–105 (1997). DOI: 10.1161/01.cir.96.1.99
[23] J. Zhang, Y. Fan, Y. Song, J. Xu. Medicine, **97** (34), e12022 (2018). DOI: 10.1097/MD.0000000000012022
[24] B. Yakimov, E. Shirshin, J. Schleusener, A. Allenova, V. Fadeev, M. Darvin. Sci. Rep., **10** (1), 14374 (2020). DOI: 10.1038/s41598-020-71220-6
[25] A. Sdobnov, M. Darvin, J. Schleusener, J. Lademann, V. Tuchin. J. Biophotonics, **12** (5), e201800283 (2018). DOI: 10.1002/jbio.201800283
[26] A. Cios, M. Ciepielak, Ł. Szymański, A. Lewicka, S. Cierniak, W. Stankiewicz, M. Mendrycka, S. Lewicki. Int. J. Mol. Sci., **22** (5), 2437 (2021). DOI: 10.3390/ijms22052437
[27] I. Bratchenko, L. Bratchenko, A. Moryatov, Y. Khristoforova, D. Artemyev, O. Myakinin, A. Orlov, S. Kozlov, V. Zakharov. Experimental Dermatology, **30** (5), 652–663 (2021). DOI: 10.1111/exd.14301
[28] Z. Wu, B. Deng, Y. Zhou, H. Xie, Y. Zhang, L. Lin, J. Ye. Advanced Science, **10** (24), 2301721 (2023). DOI: 10.1002/advs.202301721
[29] E. Rimskaya, S. Shelygina, A. Timurzieva, I. Saraeva, E. Perevedentseva, N. Melnik, K. Kudrin, D. Reshetov, S. Kudryashov. Int. J. Mol. Sci., **24** (19), 14748 (2023). DOI: 10.3390/ijms241914748
[30] Z. Movasaghi, S. Rehman, I.U. Rehman. Appl. Spectroscopy Rev., **42** (5), 493–541 (2007). DOI: 10.1080/05704920701551530
[31] C. Choe, J. Lademann, M.E. Darvin. Analyst, **141** (22), 6329–6337 (2016). DOI: 10.1039/C6AN01717G
[32] F. León-Bejarano, M.O. Méndez, M.G. Ramírez-Elías, A. Alba. Appl. Spectrosc., **73** (12), 1436–1450 (2019). DOI: 10.1177/0003702819860121
[33] N.J. Kline, P.J. Treado. J. Raman Spectroscopy, **28** (2–3), 119–124 (1997). DOI: 10.1002/(SICI)1097-4555(199702)28:2/3¡119::AID-JRS73¿3.0.CO;2-3
[34] C. Camerlingo, I. Delfino, G. Perna, V. Capozzi, M. Lepore. Sensors, **11** (9), 8309–8322 (2011). DOI: 10.3390/s110908309

Translated by E.Ilinskaya